Journal of Inorganic and Organometallic Polymers and Materials (2023) 33:1134–1146
https://doi.org/10.1007/s10904-023-02563-6

RESEARCH

Synthesis and Characterization of Composite Film Based on Cellulose of Napier Grass Incorporated with Chitosan and Gelatine for Packaging Material

T. N. Tuan Rohadi[1,2] · M. J. M. Ridzuan[1] · M. S. Abdul Majid[1] · A. Azizan[1] · Fauziah Mat[1] · S. M. Sapuan[3]

Received: 21 November 2022 / Accepted: 26 January 2023 / Published online: 4 February 2023

Abstract

Mitigating environmental pollution, which adversely affects humans, wildlife, and habitat, has been attracting increasing attention worldwide, especially with reference to the importance of using composite films. In this study, composite films consisting of cellulose, chitosan, and gelatine were analysed and characterized. It was fabricated via a solution casting method. The cellulose extracted from the whole stem, cortex, and pith of Napier grass with 4, 8, 12, and 16% alkali concentrations were used to produce the composite films. Based on the thermogravimetric analysis, mechanical analysis, Fourier-transform infrared spectroscopy (FTIR) analysis, X-ray diffraction (XRD) analysis, and scanning electron microscopy (SEM) observation, it was confirmed that the interaction of cellulose of Napier grass, chitosan and gelatine had improve the thermal behaviour, strength, composition, crystallinity, and morphology of composite films. The composite films using 8% alkali-treated cellulose from the whole stem had an ordered structure with $2\theta = 22.68°$. Furthermore, it contained the highest final residue (74.85%) and tensile strength of 4.58 ± 0.373 MPa.

Keywords Chitosan · Cellulose · Composite films · Gelatine · Napier grass

1 Introduction

The packaging materials ability to demonstrate the various functions expected had increased consumer demands [1]. Additionally, healthcare facilities, particularly those with surgical departments, prefer packaging materials such as sterilisation wraps, wrapped perforated instrument cassettes, and plastic or paper peel pouches to preserve the sterility of the processed item after sterilization [2]. Meanwhile, packaging materials derived from petrochemical sources are widely used in our daily lives, industries, and other commercial sectors because of their high performance and low cost of production [3, 4]. However, these petrochemical sources make this type of packaging materials non-biodegradable and unsustainable, thereby leading to environmental pollution, which adversely affects humans, wildlife, and habitat [2]. In this regard, packaging materials should be designed that aiming to reduce environmental pollution which can represent an additional asset in innovative packaging [1]. Therefore, this issue has increased worldwide awareness, as well as highlight the importance of using biodegradable packaging material fabricated from renewable resources and natural materials [5].

✉ M. J. M. Ridzuan
ridzuanjamir@unimap.edu.my

T. N. Tuan Rohadi
tuannurain96@gmail.com

M. S. Abdul Majid
shukry@unimap.edu.my

A. Azizan
azisyahirah@unimap.edu.my

Fauziah Mat
fauziah@unimap.edu.my

S. M. Sapuan
sapuan@upm.edu.my

[1] Faculty of Mechanical Engineering & Technology, Universiti Malaysia Perlis (UniMAP), Perlis, Malaysia

[2] Faculty of Electronic Engineering & Technology, Universiti Malaysia Perlis (UniMAP), Perlis, Malaysia

[3] Department of Mechanical and Manufacturing Engineering, Faculty of Engineering, Universiti Putra Malaysia, Selangor, Malaysia

The natural materials, such as chitosan, gelatine and cellulose are renewable materials under agrobiopolymers [6]. They have excellent potential as they are biodegradable, economically advantageous, and environmentally friendly [7]. Nevertheless, the resilient cohesive energy density of polymers in chitosan and gelatine has limited the mechanical properties of packaging material [8]. According to Jahit et al. [9], gelatine-based films are thermally unstable, brittle, susceptible to cracking, and provide an inadequate water barrier because of their hydrophilic nature. However, gelatine also possess exceptional cell adhesion, proliferation, and differentiation properties [10]. Besides, chitosan exhibits high degradation rate and antimicrobial in nature, but it is also possessing a low mechanical strength [10].

Another widely used natural polymer is cellulose [11]. Cellulose-based film is mainly cellulose esters and derivatives, such as cellulose acetate (CA), nitrocellulose, and celluloid [12]. However, CA is expensive and derived using a high concentration of acetic anhydride or sulfuric acid, which is environmentally detrimental [12]. Likewise, to replace the CA, the development of new cellulose-based films from waste crops, such as pineapple [13], oil palm [14], and durian rind [15] were also reported earlier. Notably, the cellulosic feedstock by Napier grass (NG), which scientific name is *Pennisetum Purpureum,* can serve as an alternative material for composite film reinforcement materials [16]. Other than that, NG also is a part of a push–pull agricultural pest management strategy as it requires less water and nutrients [16]. Additionally, the cortex and pith of NG represent 84% and 16%, respectively, which can optimise the use of the NG stem for packaging material fabrication. Consequently, this can decrease the dependence on petrochemical sources in packaging material production [2].

Therefore, several researchers have tried to combine the beneficial properties by combining of other fillers with chitosan and gelatine which showed a good mechanical strength, more rigid and microbial protection in film [9, 17–19]. In previous study, the research done by Kumar et al. [18, 19] showed that the nano-composite films incorporating silver with chitosan and gelatine had improved microbial protection. However, the research done by Sharma et al. [10] had observed that the ternary nano-biocomposite films using bacterial cellulose with implementation of chitosan and gelatine had produced more rigid and higher mechanical properties of the films. Accordingly, it would be expected for good combination of chitosan, gelatine and cellulose for this research as demonstrated by Sharma et al. [10].

Hence, it has become an interesting reason to develop composite films incorporated with cellulose, chitosan, and gelatine. Furthermore, no previous study has investigated the interaction of cellulose, chitosan, and gelatine in the composite films using the whole stem, cortex, and pith of NG. In addition, an ideal percentage concentration of alkali treatment for cellulose extraction also can improve the characteristics of composite films. According to a previous paper, the cellulose extracted from the whole stem, cortex and pith of NG at 4, 8, 12, and 16% concentrations of NaOH treatment had a significant impact on the thermal properties, as well as the chemical composition, morphology, and crystallinity of the material [20].

As a result, in this case study, an in-depth investigation of the effect of different alkali concentrations cellulose filler loading in the composite films was conducted. The cellulose filler from the whole stem, cortex, and pith of Napier grass for cellulose extraction using 4, 8, 12, and 16% concentration of alkali treatment was used in the composite film's fabrication. The thermogravimetric analysis (TGA), mechanical properties, Fourier-transform infrared spectroscopy (FTIR), X-ray diffraction (XRD), and scanning electron microscopy (SEM) studies of the composite films fabricated were investigated. The incorporation of different cellulose extracts, chitosan, and gelatine in composite films could produce different thermal, chemical composition, crystallinity, morphological, and strength results.

2 Materials and Methods

2.1 Material Preparation

Napier grass (NG), scientifically known as *Pennisetum Purpureum*, is harvested from a local plantation in the northern peninsula of Malaysia. The NG stems were extracted to separate the cortex and pith, which represented the outer and inner parts of the NG stem, respectively. Subsequently, the cellulose was prepared through the alkali and bleaching treatments of the whole stem, cortex and pith of NG, as explained in a previous study [20]. Prior to the separation process, the total weight of each NG stem was measured and separated to 84% of the cortex and 16% of the pith [21]. The dried whole stem, cortex and pith of NG were ground and sieved to obtain a powdered form. The prepared whole stem, cortex and pith of NG powder were then labelled as WNG, CNG, and PNG, respectively. Cellulose was extracted from the WNG, CNG, and PNG at 4, 8, 12, and 16% concentrations of sodium hydroxide (NaOH), followed by a 1.7% concentration of sodium chlorite ($NaClO_2$). The cellulose extracted from the WNG, CNG, and PNG were used as base materials in the composite film's preparation. The NaOH, $NaClO_2$, chitosan, acetic acid, gelatine, and glycerol were obtained from Sigma-Aldrich, Germany.

2.2 Composite Films Preparation

The composite film was prepared from two types of solutions using the casting method. Primarily, two solutions were

prepared and named as the first and second solutions. For the first solution, the chitosan was mixed with 2% (v/v) acetic acid in 100 mL for 12 h using a magnetic stirrer. In the second solution, the gelatine was dissolved in 100 mL of water at room temperature. Prior to the preparation of the composite film suspension, 1 g of 4, 8, 12, and 16% alkali-treated cellulose of WNG, CNG, and PNG were added to 40 mL of the second solution. The mixture solutions were then further stirred for 12 h without heating. Subsequently, 60 mL of the first solution was added to the mixture solution and stirred for 30 min. In the following step, 1 mL of glycerol was added to the mixture and stirred for 2 h. Consequently, 12 different types of composite film suspension from the 4, 8, 12, and 16% alkali-treated cellulose of WNG, CNG, and PNG were obtained. The composite films were fabricated by pouring 30 mL of the composite film suspension into a 120 mm diameter glass petri dish and evaporating at room temperature for 24 h. Finally, the composite films for the 4, 8, 12, and 16% alkali-treated cellulose of WNG, CNG, and PNG were then peeled off from the petri dishes.

2.3 Thermogravimetric Analysis (TGA)

The TGA was performed using TGA-50 (Shimadzu, Japan) to evaluate the decomposition and thermal stability of the composite films. The composite films were gradually heated from room temperature to 600 °C at a heating rate of 10 °C/min with a flow rate of 20 mL/min [22].

2.4 Tensile Test

Tensile strength tests were tested using a micro universal testing machine according to the ASTM D882-02 standard. The composite films with the dimension of 75 mm in length and 16 mm in width. The crosshead speed was fixed at 2 mm/min. The average thickness of the composite film's samples ranged from 0.09 to 0.23 mm. The tensile strength test was repeated five times to obtain an average tensile strength value. The tensile strength was determined using the following equation [23]:

$$\text{Tensilestrength} = \frac{\text{Load(N)}}{\text{Areaofsamplethickness(mm}^2\text{)}} \quad (1)$$

2.5 Fourier-Transform Infrared (FTIR) Spectroscopy

The FTIR analysis of the composite films were performed using an FTIR spectrophotometer (Model: Perkin Elmer). The spectrum for each sample was recorded with 16 scans in the frequency range from 4000 to 400 cm^{-1} with a resolution of 4 cm^{-1}. The FTIR spectra were used to determine the presence of functional groups and interactions between cellulose, chitosan, and gelatine in the composite films [18, 19].

2.6 X-Ray Diffractometer (XRD)

The crystalline structure of the composite film was investigated using the X-ray diffractometer (Model: Aeris benchtop, Malvern PANalytical Ltd., United Kingdom). The instrument operated at a voltage of 40 kV and a tube current of 250 mA with Cu Kα radiation (λ = 1.54 Å) for XRD analysis. The data were recorded within the scattering angles ranging from 2θ = 5–40° at a scanning rate of 5°/min. The X-ray diffraction-based Segal Crystallinity Index (CI) was calculated for simulated different sizes of crystallites for cellulose I and II [24, 25].

2.7 Scanning Electron Microscopy (SEM)

A scanning electron microscope (Model: JEOL JSM 820 microscope) was used to record the surface morphologies of samples. Scanning electron microscopy analysis was conducted to study the molecular structure, morphological surface, and transversal sections of the composite films. The images were collected at a magnification of ×500 with the beam energy in the range of 10–25 kV.

3 Results and Discussion

3.1 Thermogravimetric Analysis (TGA)

The TGA curves of the composite films for 4, 8, 12, and 16% alkali-treated cellulose of WNG, CNG, and PNG are displayed in Fig. 1a–c. The percentage of the final residues at 600 °C, as well as the initial and final degradation temperatures were calculated and tabulated in Table 1. The TGA was performed to examine the influence of cellulose on the thermal stability of the composite films. From Fig. 1 and Table 1, it is evident that the composite films prepared with 4% alkali-treated cellulose improves the thermal stability compared to that fabricated using 8% alkali-treated cellulose of WNG, CNG, and PNG. These degradation trends, which are almost similar to the those of a previous research that entails a three-step decomposition mechanism process [26], are presented in Fig. 1.

From the TGA curves in Fig. 1a–c, it was observed that the weight loss was initiated at a temperature range of 25–150 °C, which was less than 15 wt%. The first weight loss was due to the evaporation of absorbed moisture and removal of volatile compounds in the composite films [27, 28]. This could also be explained by biopolymers and glycerol being hygroscopic substances, depending on the ambient conditions [29]. In the second stage, the mass

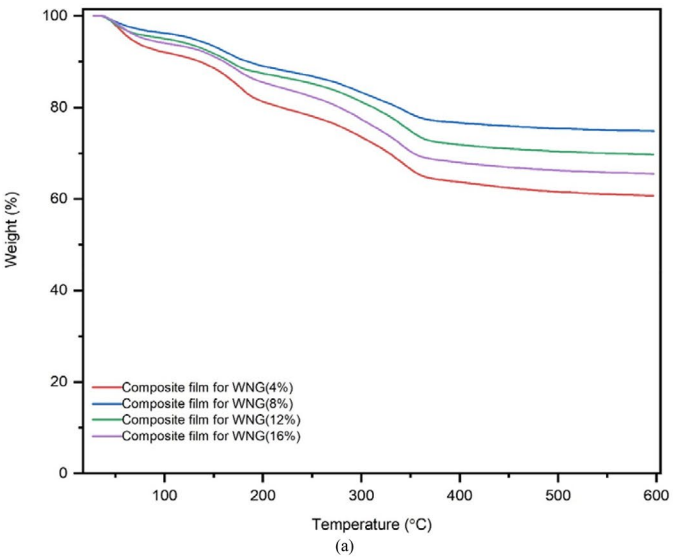

Fig. 1 TGA of composite films for cellulose of **a** WNG, **b** CNG, and **c** PNG which were treated with different alkali concentrations

Table 1 Final residues, along with the initial and final degradation temperatures of the composite films for cellulose of WNG, CNG, and PNG

Composite films sample	Initial degradation temperature (°C)	Final degradation temperature (°C)	Final residue (%)
Composite film for WNG (4%)	35.22	597.03	60.75
Composite film for WNG (8%)	36.93	597.53	74.85
Composite film for WNG (12%)	36.83	596.90	69.70
Composite film for WNG (16%)	33.62	597.37	65.50
Composite film for CNG (4%)	30.48	599.27	35.30
Composite film for CNG (8%)	29.37	597.87	39.65
Composite film for CNG (12%)	32.87	598.77	53.90
Composite film for CNG (16%)	32.46	597.19	66.10
Composite film for PNG (4%)	32.73	599.00	32.03
Composite film for PNG (8%)	25.96	597.28	35.45
Composite film for PNG (12%)	41.68	599.37	42.30
Composite film for PNG (16%)	38.67	597.55	56.65

loss at temperatures between 150 and 250 °C could be associated with the plasticizer evaporation following the thermal degradation of hemicellulose [28]. The samples were rapidly decomposed with a mass loss of 20–40 wt% in the second stage [26]. The final weight loss beyond 250 °C was attributed to the depolymerisation of the composite films material [26]. In addition, the cellulose and lignin were decomposed and caused the char formation effect [28]. As shown in Fig. 1a–c, the composite films using the cellulose of WNG, CNG, and PNG, the weight loss associated with the decomposition of cellulose started at approximately 300 °C. These shows that mass loss was dependent on the type of cellulose filler and presence of glycerol [30].

As shown in Table 1, the composite films for the 8% alkali-treated cellulose of WNG had the highest final residues for WNG samples (74.85%). Thereafter, it was followed by the composite films for the 16% alkali-treated cellulose of CNG, which had the highest final residues for CNG samples (66.1%). For the PNG samples, the composite films for the 16% alkali-treated cellulose of PNG had the highest final residues (56.65%), indicating that the implementation of different concentration of the NaOH treatment process for cellulose isolation would affect the interaction between cellulose, chitosan, and gelatine. Hence, this also shows that the composite films for the 8% alkali-treated cellulose of WNG can resist thermal degradation at high temperatures compared to the composite films for the 16% alkali-treated cellulose of CNG and PNG. The overall results of the thermal properties of the composite films for the 4, 8, 12, and 16% alkali-treated cellulose of WNG, CNG, and PNG showed that the weight loss ranged from 35 to 75% in a range of 50 to 600 °C [27, 31].

3.2 Tensile Strength

The tensile strengths of the composite films for the 4, 8, 12, and 16% alkali-treated cellulose of WNG, CNG, and PNG are presented in Fig. 2. Based on Fig. 2b and c, it is evident that the incorporation of chitosan, gelatine, and cellulose significantly increased the tensile strength of the composite films for the 4, 8, 12, and 16% alkali-treated cellulose of CNG and PNG. Meanwhile, for the WNG samples in Fig. 2a, the composite films for the 8% alkali-treated cellulose of WNG had the highest tensile strength (4.58 ± 0.373 MPa). Based on these results, the presence of crystallisation fillers in the films causes the molecular bond in the interaction between chitosan and gelatine to become stronger [32, 33]. According to previous studies, gelatine- and chitosan-based films are brittle and susceptible to cracking owing to the resilient cohesive energy density of the polymer [8, 9]. Nevertheless, Muhammad et al. [33] proposed that the trend of the tensile strength gradually increases with the addition of cellulose as fillers. Therefore, the alkaline treatments during isolation process had improved the tensile strength to sustain a high load in application [34]. This may be due to the changes in the cellulose crystallinity during the isolation process, which involves the removal of the weak amorphous component [34].

Additionally, the mechanical properties in the composite films were found to improve owing to the removal of the hemicellulose and lignin in cellulose of WNG at an appropriate concentration [33]. In addition, stronger –OH interactions between the filler and glycerol cause plasticisation [35]. When glycerol is incorporated into the cellulose, chitosan, and gelatine mixture, hydrogen bonding with glycerol is formed [36]. Consequently, direct interactions between mixtures were reduced, allowing the polymer chains to

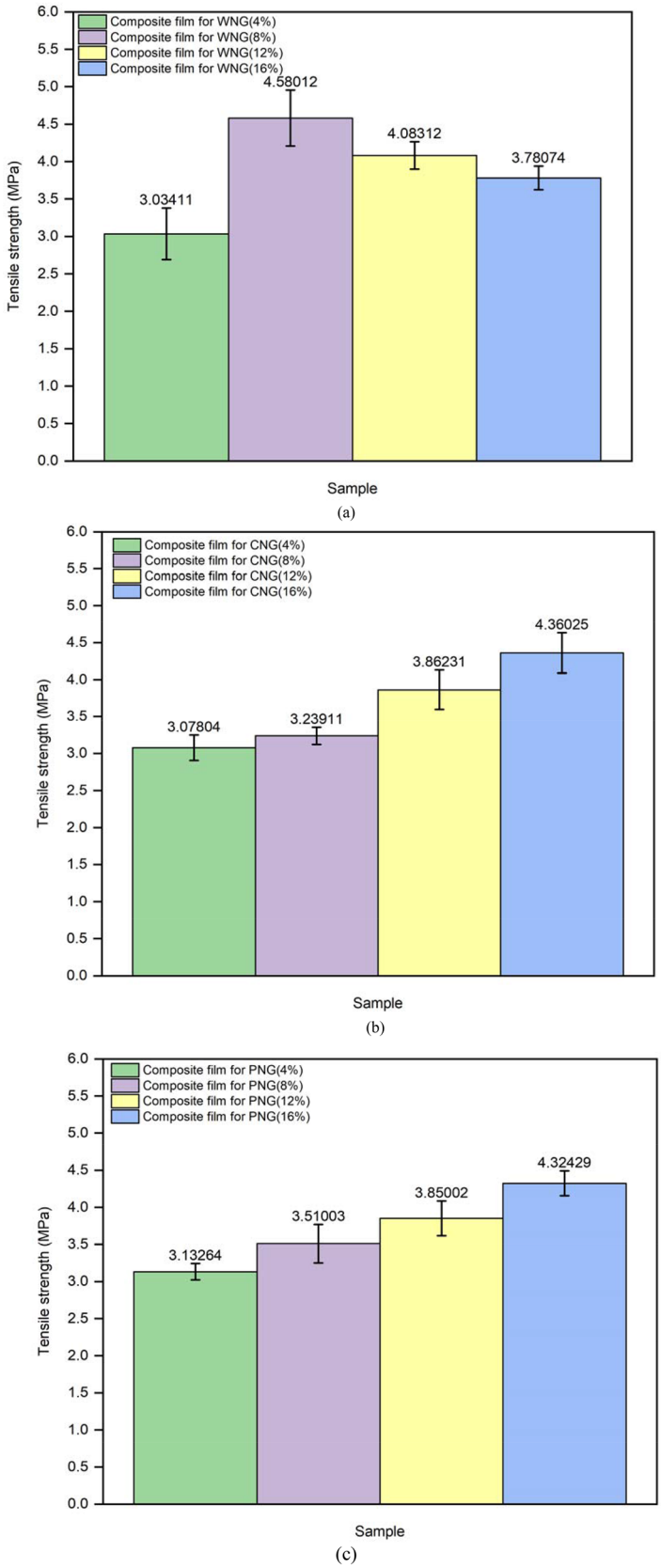

Fig. 2 Tensile strength for the composite films using the cellulose of **a** WNG; **b** CNG and **c** PNG, treated with different alkali concentrations

move freely [32]. However, as shown in Fig. 2a, the tensile strength of the composite films for the 12 and 16% alkali-treated cellulose of WNG was significantly decreased to 4.08 ± 0.183 and 3.78 ± 0.158 MPa, respectively. This may be due to the uneven distribution of the filler may cause the composite films to be inhomogeneous in one area, as shown in the SEM micrograph. Besides, the filler orientation and variation in the size of fillers also may affects the mechanical strength of composite films [28, 37]. Notably, the composite films using the cellulose of WNG consists of a variation in the size of the filler owing to the mixture of the CNG and PNG. The cellulose of CNG, which has a smaller diameter, may cause it to be distributed randomly inside the composite films [37].

Overall, the results of this study indicate that the removal of hemicellulose and lignin at the appropriate concentration for the production of composite films can have a positive effect on the mechanical characteristics and interaction of chitosan, gelatine, and cellulose [38]. Compared to the composite films using the cellulose of WNG, CNG, and PNG, the composite films for the 8% alkali-treated cellulose of WNG had the highest tensile strength (4.58 ± 0.373 MPa), followed by the composite films for the 16% alkali-treated cellulose of CNG (4.36 ± 0.273 MPa), and the composite films for the 16% alkali-treated cellulose of PNG (4.32 ± 0.167 MPa). Therefore, the results demonstrate that the composite films using the alkali-treated cellulose has sufficient tensile strength for biodegradable packaging [18, 19].

3.3 Fourier-Transform Infrared (FTIR) Spectroscopy

The FTIR spectra of the composite films for the 4, 8, 12, and 16% alkali-treated cellulose of WNG, CNG, and PNG are shown in Fig. 3. From Fig. 3a–c, it is evident that the common bands observed at 3260–3390, 2910–2940, 1630–1644, and 1030–1041 cm^{-1} are attributed to O–H, C–H, C=O, and C–O absorption peaks, respectively [39]. The presence of these four major absorption peaks in the FTIR spectra of the composite films for 4, 8, 12, and 16% alkali-treated cellulose of WNG, CNG, and PNG displayed the formation of the biodegradable composite films [33]. Based on Fig. 3,the peaks at 3260–3390 cm^{-1} show that the hydrogen bond formation in the pendant and hydroxyl groups, such as NH_2 and OH of the carbohydrate structure occurred because of the complex vibrational stretching [18, 19, 40]. The broadening of the O–H groups also can occur owing to the interaction of cellulose with gelatine and chitosan [26].

In addition, the common bands observed at 2910–2940 cm^{-1} were due to the C–H stretching vibrations of the methyl and methylene groups (CH_2) in the chitosan chain [18, 19, 41]. The other common peak at 1630–1644 cm^{-1} was attributed to the adsorption of water and the bending peaks of the C=O and C=C bonds, which

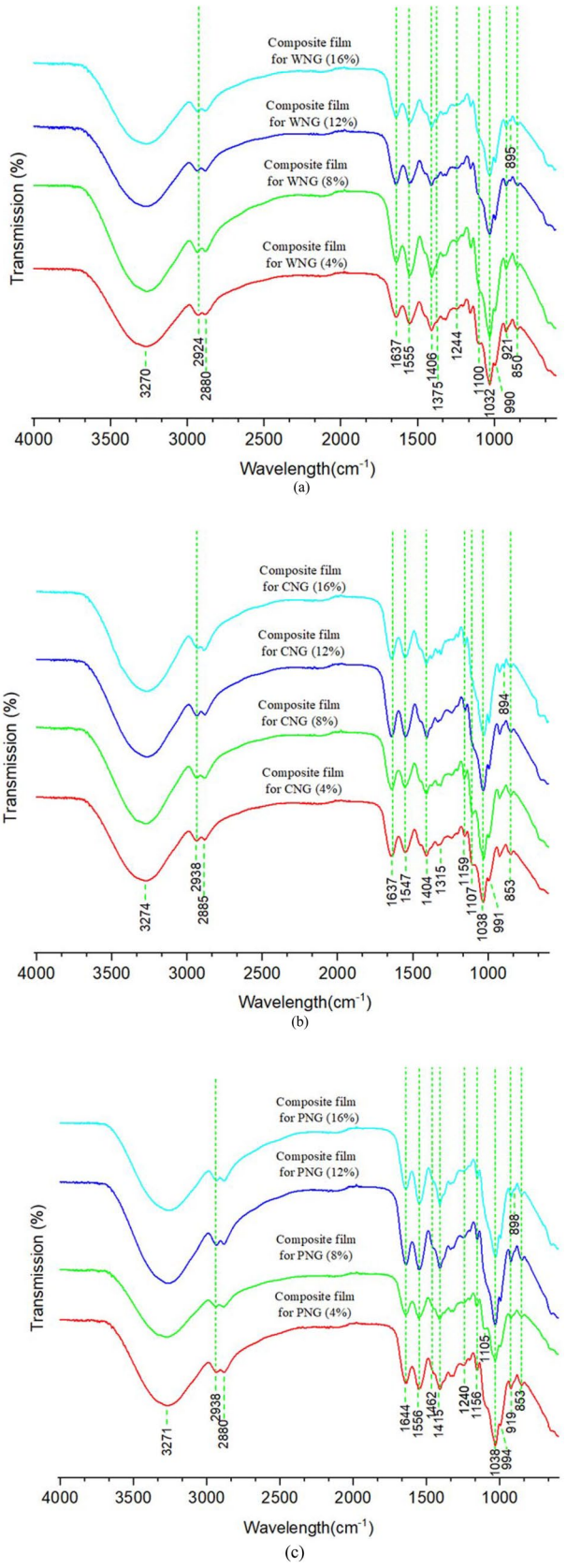

Fig. 3 FTIR for the composite films using the cellulose of **a** WNG; **b** CNG, and **c** PNG, treated with different alkali concentrations

were not found in polysaccharides [18, 19, 41]. Additionally, this peak may also be associated with the groups participating in the bonds formed between cellulose, chitosan, and gelatine interactions [41, 42]. Moreover, based on Fig. 3, it can be observed that the wavelength at 1000–1260 cm^{-1} represents the C–O bending of the C–O–H group and C–O–C stretching linkage of polysaccharide chains [41, 43]. The rings, which are bound together with the C–O–C bond, are also known as the glycosidic bond [44]. The change in crystallinity of the cellulose result was due to the changes in the CH_2 symmetrical bending vibration and glycosidic linkage [44]. Therefore, the addition of cellulose extracted with a higher concentration alkali treatment can enhance the effect of the interaction mechanism between the molecular structure of chitosan and gelatine in the production of composite films [18, 19].

Furthermore, the alteration in characteristic absorption band frequency and intensity possibly indicated the role of cellulose in strengthening composite films networks [32]. From Fig. 3a–c, it can be observed that the absorption bands for the composite films using the 4% alkali-treated cellulose of WNG, CNG, and PNG were 2924, 2938, and 2938 cm^{-1}, respectively. The absorption band continued to shift to a lower wavenumber for the composite films for the 8, 12 and 16% alkali-treated cellulose of WNG, CNG, and PNG. These results showed that a more stable and stronger hydrogen bonding exists when using cellulose in composite films production [33]. This also show that cellulose at higher concentration alkali treatment does not affect the molecule in composite films production [33]. Consequently, this decreased the free space in the composite films network and strengthened the composite films structure [45]. Hence, the ability of water and oxygen resistance of composite films was improved [45]. Overall, the FTIR results demonstrated that the quality of the composite films from the cellulose of WNG, CNG, and PNG production was good, exhibiting an improvement in chemical composition due to the incorporation of different cellulose extracts, chitosan, and gelatine in composite films.

3.4 X-Ray Diffractometer (XRD)

The composite films for the 4, 8, 12, and 16% alkali-treated cellulose of WNG, CNG, and PNG are shown in Fig. 4. Based on Fig. 4a–c, it is evident that a new strong characteristic reflection appeared from the diffraction patterns of the composite films at around $2\theta = 12°$, 15°, 20°, or 22°, which indicate a crystalline structure [25]. Moreover, Fig. 4a–c shows that the composite films for the 4% and 8% alkali-treated cellulose of WNG, CNG, and PNG mainly exhibited two diffraction peaks at around $2\theta = 15°$ (broad) and 22° (sharp and intense) indicating the cellulose I structure which corresponded to the ((1–10), (110), and (200)) crystal plane [18, 19, 46]. Meanwhile, the composite films for the 12 and 16% alkali-treated cellulose of WNG, CNG, and PNG mainly exhibited three diffraction peaks at around $2\theta = 12°$ (small and sharp), 20° (broad and intense), and 22° (sharp and intense), indicating the cellulose II structure which corresponded to the ((1–10),(110), and (020)) crystal plane [4, 18, 19, 46]. This indicates that the crystalline structures of the composite films can be affected by cellulose filler added as different percent of alkali concentration used during the isolation treatment process [44].

Furthermore, the numerical values of the Crystallinity Index (CI) for the different composite films are shown in Table 2. Table 2 also shows that the degrees of diffraction angle for the composite films using 4, 8, 12, and 16% alkali-treated cellulose of WNG, CNG, and PNG were completely different from each other. These findings shows that the presence of cellulose, chitosan and gelatine has affected the preferred intensity at diffraction peaks but not the diffraction patterns of the composite films. Thus, the value of CI for the composite films had decreases due to the mixed of chitosan, gelatine and the cellulose extracted from the whole stem, cortex and pith of NG at 4, 8, 12, and 16% concentrations of NaOH treatment [20]. This was due to the change in the upper angle specified a decrease in the subsequent interlayer spacing, which signifies that a mixed component has occurred in the composite films [26]. Besides, from Fig. 4a–c, it can be observed that the composite films using the 8% alkali-treated cellulose of WNG had the highest value: $2\theta = 22.68°$, indicating that it had the most ordered structure among the composite films [26]. This indicated that the cellulose was uniformly dispersed in the composite films and built a strong interaction with chitosan and gelatine [45]. Overall, the XRD studies demonstrate that composite films can change their amorphous arrangement when the alkali-treated concentration of cellulose increases.

3.5 Scanning Electron Microscopy (SEM) Observation

The differences between the physical structure of the composite films for the 4, 8, 12, and 16% alkali-treated cellulose of WNG, CNG, and PNG are shown in Fig. 5. The physical structure of the composite films became flexible and smoother as the alkali treatment concentration increased. Thus, the objective of fabricating composite films from agricultural and food wastes to replace petrochemical source was achieved.

The SEM was used to observe the morphology and cross-sectional structure of the composite films. The SEM micrographs of the composite films for the 4, 8, 12, and 16% alkali-treated cellulose of WNG, CNG, and PNG surfaces are shown in Fig. 6.

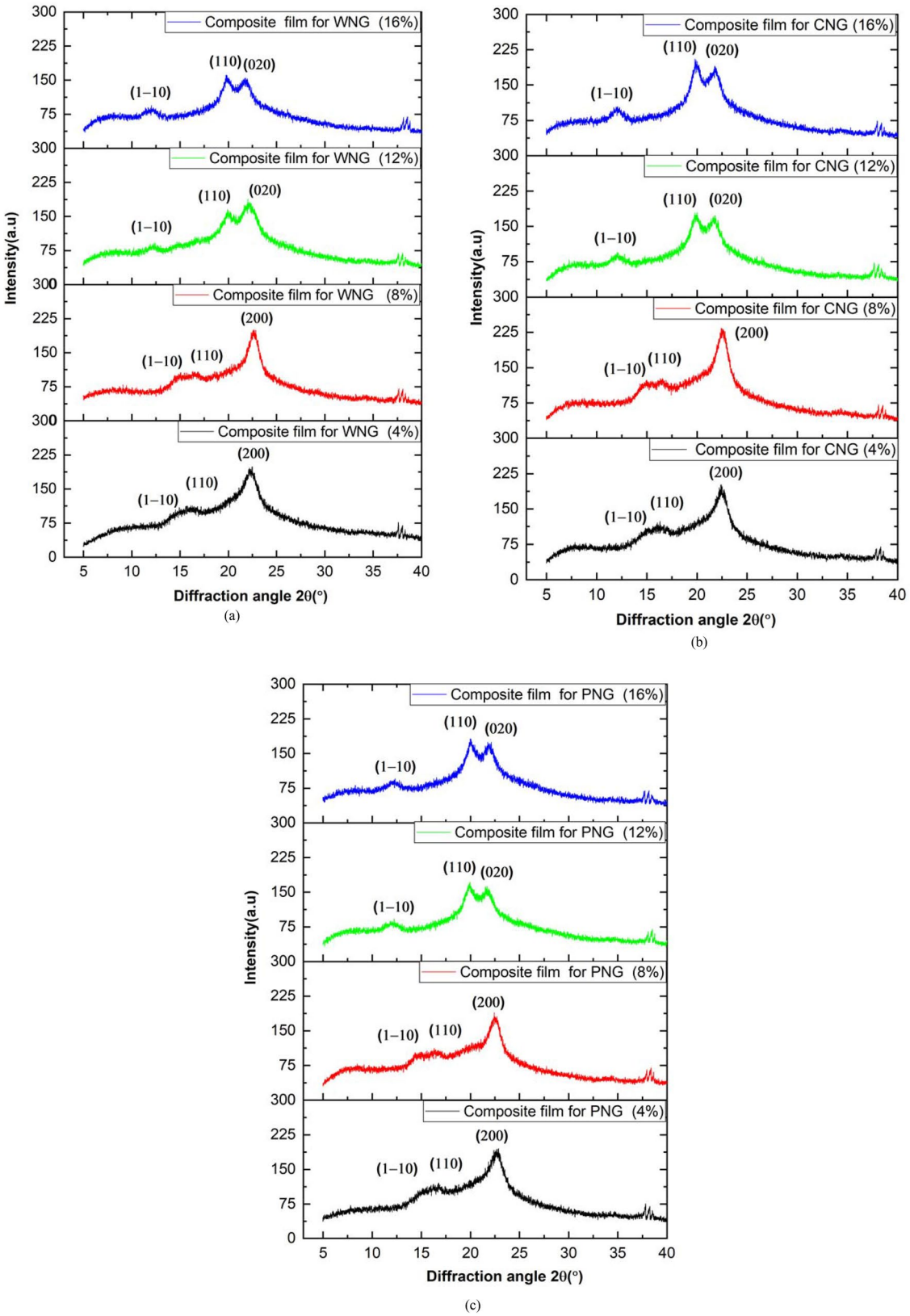

Fig. 4 XRD for the composite films for the 4, 8, 12, and 16% alkali-treated cellulose of **a** WNG; **b** CNG; and **c** PNG

Table 2 X-ray diffraction (XRD) results for the composite films synthesized using cellulose of WNG, CNG, and PNG

Composite films sample	2θ at minimum (°)	Minimum intensity	2θ at highest diffraction peak (°)	Intensity of highest peak	CI (%)
Cellulose I					
Composite film for WNG (4%)	17.62	90.71	22.19	227	60.04
Composite film for WNG (8%)	17.76	85.29	22.68	226	62.26
Composite film for CNG (4%)	17.34	90.71	22.37	235	61.4
Composite film for CNG (8%)	17.43	91.43	22.47	278	67.11
Composite film for PNG (4%)	17.54	95.71	22.56	214	55.28
Composite film for PNG (8%)	17.71	87.43	22.56	208	57.97
Cellulose II					
Composite film for WNG (12%)	13.23	66.71	19.9	217	69.26
Composite film for WNG (16%)	13.71	60.29	21.68	183	67.05
Composite film for CNG (12%)	13.48	64.14	20	204	68.59
Composite film for CNG (16%)	13.83	68.57	19.77	227	69.79
Composite film for PNG (12%)	13.67	62.43	19.9	199	68.63
Composite film for PNG (16%)	14.07	66.29	20.08	198	66.52

From the SEM results, it can be seen that there is a difference in the cellulose structure of the composite films for the 4, 8, 12, and 16% alkali-treated cellulose of WNG, CNG, and PNG. Based on Fig. 6a–c, the SEM micrographs of the composite films for the 8% alkali-treated cellulose of WNG, CNG, and PNG showed a fluctuating, continuous structure, and better compatible morphology without cavities, edges, and holes [47]. Besides, Fig. 6c also demonstrates that the composite films for the 12 and 16% alkali-treated cellulose of PNG consisted of cellulose structures similar to twisted ropes tied to each other [12]. Thus, it confirmed the superior bonding among components, which was attributed to the existence of chemical interactions between cellulose, chitosan, and gelatine [47]. In addition, the added glycerol helped make a homogenous mixture with clear signs of plasticisation in the composite films with a smoother surface morphology [26]. This may be owing to the biomass composition and interactions between cellulose, chitosan, and gelatine in the composite films.

However, from Fig. 6a and c, the composite films using the 4% alkali-treated cellulose of WNG, and PNG shows that the multicellular structures of filler were present. Besides, the filler-pulled-out propagations in the composite films indicate poor bonding among the components [27]. Moreover, it can be observed from Fig. 6a that the composite films for the 12 and 16% alkali-treated cellulose of WNG had cellulose structures with various diameters twisted to each other [32]. Thus, this cause some voids on the surface and result in poor tensile properties [27]. Furthermore, the composite films using the 12 and 16% alkali-treated cellulose of CNG shows poor interfacial adhesion on the surface morphology as a result of the non-homogeneity of the composite films. The lack of a solvent interaction in the solution casting process might be the reason for the resulting structure and the poor homogenisation of chitosan and gelatine [38]. This is because incompatible mixtures would reflect the porosity of a specific surface area [32]. Overall, the results indicated that composite films using the 8% alkali-treated cellulose from NG exhibited a homogeneous structure on its surface, which proved the high quality and good architecture of the produced composite films [4].

4 Conclusions

The thermal behaviour, strength analysis, composition, crystallinity, and morphology confirmed a variation in the composite films. The results show that the addition of different concentrations of alkali-treated cellulose of WNG, CNG, and PNG in composite films can enhance the effect on its characteristics and incorporation of cellulose, chitosan, and gelatine. The presence of O–H, C–H, C=O, and C–O absorption peaks in the FTIR spectra of composite films confirmed the formation of biodegradable film. The XRD studies demonstrate that composite films can change the amorphous arrangement when the alkali-treated concentration of cellulose increases. The results also show an improvement in the thermal stability of the additional cellulose due to the strong interaction bonds formed between cellulose, chitosan, and gelatine. Overall, the incorporation between 8% alkali-treated cellulose of WNG, chitosan and gelatine had produced the most ordered structure (2θ = 22.68°) among the composite films. In addition, it had the highest final residues for composite films (74.85%), which indicated that it could resist thermal degradation at high temperatures. Thus, the study demonstrates that the NG stem has a significant potential for the industrial production of composite films.

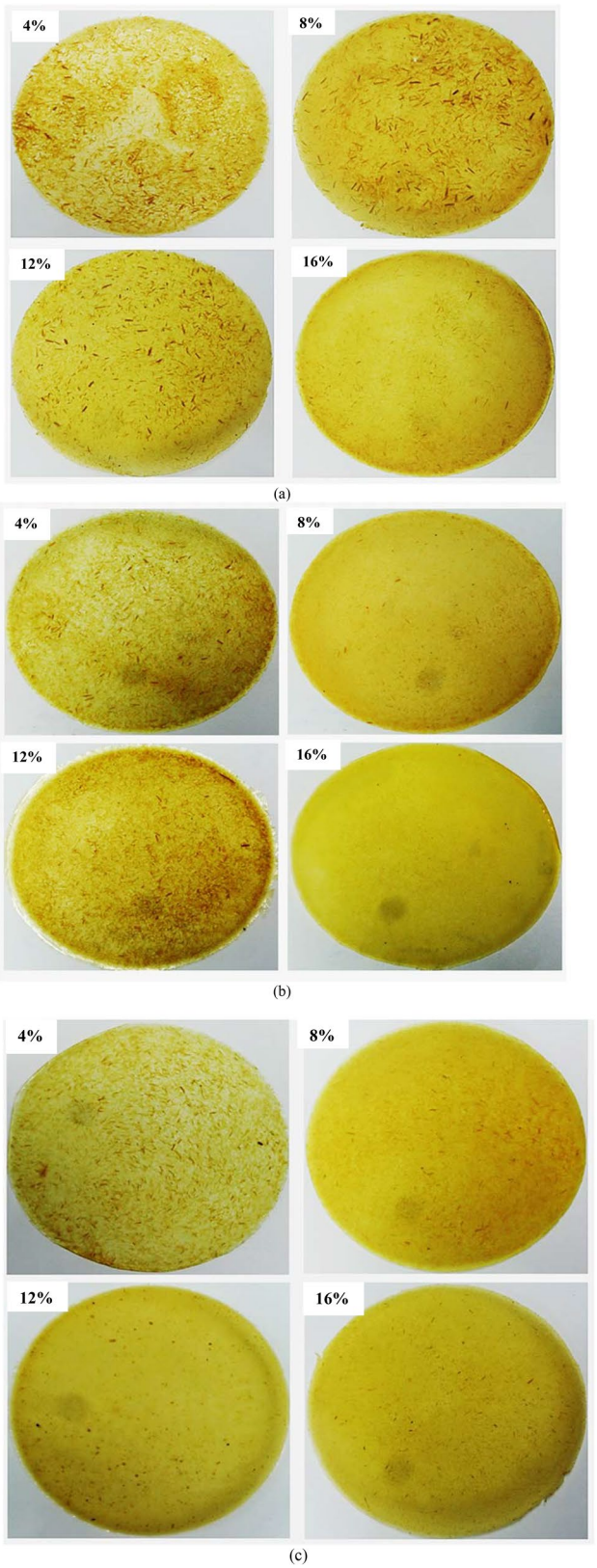

Fig. 5 Composite films for the 4, 8, 12, and 16% alkali-treated cellulose of **a** WNG; **b** CNG; and **c** PNG

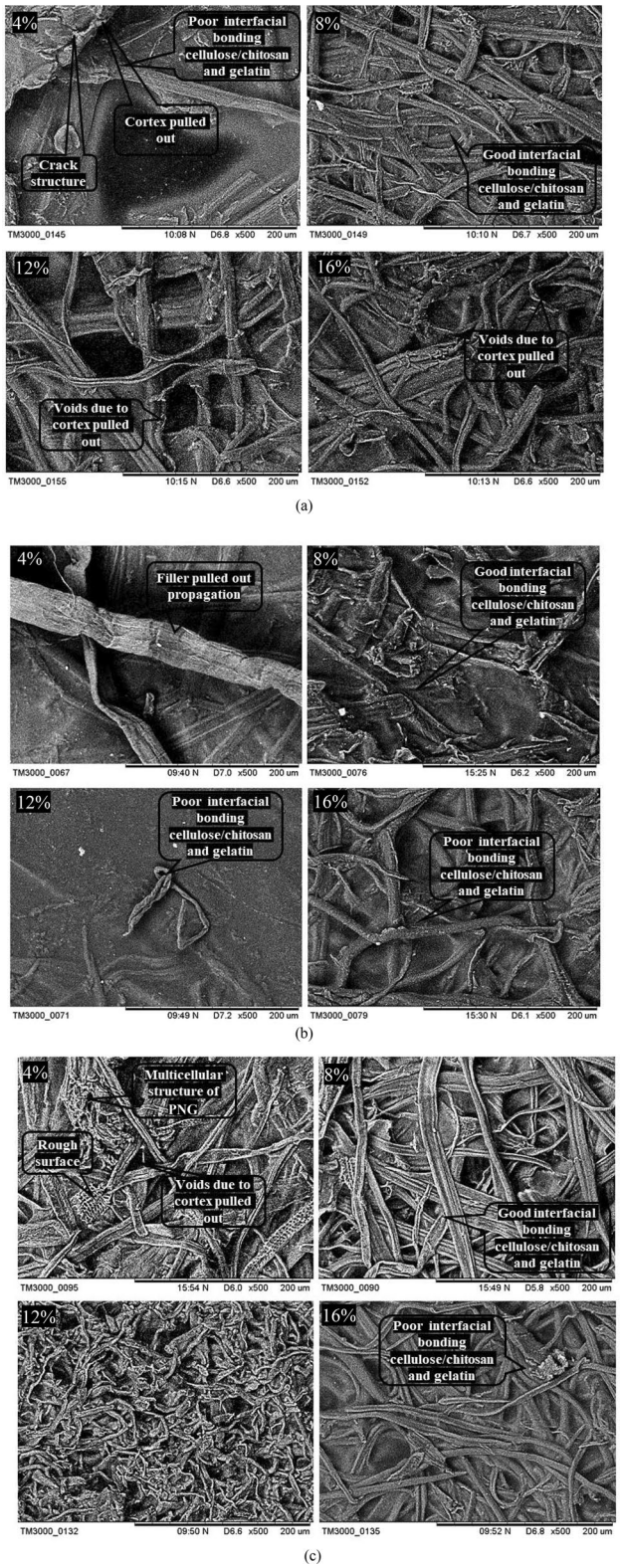

Fig. 6 SEM images of the composite films for the 4, 8, 12, and 16% alkali-treated cellulose of **a** WNG; **b** CNG; and **c** PNG

Acknowledgements The authors appreciatively thank the Universiti Malaysia Perlis (UniMAP), Universiti Teknologi Mara (UiTM) Shah Alam, and International Islamic University Malaysia (IIUM) for the support of their facility in conducting this research.

Author Contributions MJMR, TNTR and MSAM designed the entire story in this manuscript, performed all tests and data analysis. AA, FM, SMS were designed and revised the manuscript. All authors discussed the methods, results and checked the manuscripts.

Funding This work was supported by the Ministry of Education, Malaysia through the Fundamental Research Grant Scheme (Ref: FRGS/1/2020/TK0/UNIMAP/02/18).

Declarations

Conflict of interest The authors have not disclosed any competing interest.

References

1. P. Chaudhary, F. Fatima, A. Kumar, Relevance of nanomaterials in food packaging and its advanced future prospects. J. Inorg. Organomet. Polym. Mater. **30**, 5180–5192 (2020). https://doi.org/10.1007/s10904-020-01674-8
2. G. Mamatha, P. Sowmya, D. Madhuri, N. Mohan Babu, D. Suresh Kumar, G. Vijaya Charan, K. Varaprasad, K. Madhukar, Antimicrobial cellulose nanocomposite films with in situ generations of bimetallic (Ag and Cu) nanoparticles using *Vitex negundo* leaves extract. J. Inorg. Organomet. Polym. Mater. **31**, 802–815 (2021). https://doi.org/10.1007/s10904-020-01819-9
3. J. Lucenius, K. Parikka, M. Österberg, Nanocomposite films based on cellulose nanofibrils and water-soluble polysaccharides. React. Funct. Polym. **85**, 167–174 (2014). https://doi.org/10.1016/j.reactfunctpolym.2014.08.001
4. G. Zhao, X. Lyu, J. Lee, X. Cui, W.-N. Chen, Biodegradable and transparent cellulose film prepared eco-friendly from durian rind for packaging application. Food Packag. Shelf Life **21**, 100345 (2019). https://doi.org/10.1016/J.FPSL.2019.100345
5. E. Kabir, R. Kaur, J. Lee, K.H. Kim, E.E. Kwon, Prospects of biopolymer technology as an alternative option for non-degradable plastics and sustainable management of plastic wastes. J. Clean. Prod. (2020). https://doi.org/10.1016/j.jclepro.2020.120536
6. H. Haghighi, F. Licciardello, P. Fava, H.W. Siesler, A. Pulvirenti, Recent advances on chitosan-based films for sustainable food packaging applications. Food Packag. Shelf Life **26**, 100551 (2020). https://doi.org/10.1016/j.fpsl.2020.100551
7. R. Ning, M. Takeuchi, J.M. Lin, T. Saito, A. Isogai, Influence of the morphology of zinc oxide nanoparticles on the properties of zinc oxide/nanocellulose composite films. React. Funct. Polym. **131**, 293–298 (2018). https://doi.org/10.1016/j.reactfunctpolym.2018.08.005
8. S. Kumar, P. Singh, S.K. Gupta, J. Ali, S. Baboota, Biodegradable and recyclable packaging materials: a step towards a greener future, in: Encyclopedia of Renewable and Sustainable Materials (Elsevier, Amsterdam, 2020), pp. 328–337. https://doi.org/10.1016/b978-0-12-803581-8.10934-8
9. I.S. Jahit, N.N.M. Nazmi, M.I.N. Isa, N.M. Sarbon, Preparation and physical properties of gelatin/CMC/chitosan composite films as affected by drying temperature. Int. Food Res. J. **23**(23), 1068–1074 (2016)
10. C. Sharma, N.K. Bhardwaj, P. Pathak, Ternary nano-biocomposite films using synergistic combination of bacterial cellulose with chitosan and gelatin for tissue engineering applications. J. Biomater. Sci. Polym. Ed. **32**, 166–188 (2021). https://doi.org/10.1080/09205063.2020.1822122
11. M. Abdelraof, M.M. Farag, Z.M. Al-Rashidy, H.Y.A. Ahmed, H. El-Saied, M.S. Hasanin, Green synthesis of bioactive hydroxyapatite/cellulose composites from food industrial wastes. J. Inorg. Organomet. Polym. Mater. **32**, 4614–4626 (2022). https://doi.org/10.1007/s10904-022-02462-2
12. B. Rohmawati, F.A. Nata Sya'idah, R. Rhismayanti, D. Alighiri, W. Tirza Eden, Synthesis of bioplastic-based renewable cellulose acetate from teak wood (*Tectona grandis*) biowaste using glycerol-chitosan plasticizer. Orient. J. Chem. **34**, 1810–1816 (2018)
13. A.M. Mansor, J. Shiun Lim, F.N. Ani, H. Hashim, W. Shin Ho, Characteristics of cellulose, hemicellulose and lignin of MD2 pineapple biomass. Chem. Eng. Trans. **72**, 79–84 (2019). https://doi.org/10.3303/CET1972014
14. S. Rasila, A.M. Rasli, I. Ahmad, A.M. Lazim, A. Hamzah, Extraction and characterization of cellulose from agricultural residue-oil palm fronds. Malaysian J. Anal. Sci. **21**, 1065–1073 (2017)
15. P. Penjumras, R.B.A. Rahman, R.A. Talib, K. Abdan, Extraction and characterization of cellulose from durian rind. Agric. Agric. Sci. Procedia **2**, 237–243 (2014). https://doi.org/10.1016/j.aaspro.2014.11.034
16. C.A.O. Midega, J.O. Pittchar, J.A. Pickett, G.W. Hailu, Z.R. Khan, A climate-adapted push-pull system effectively controls fall armyworm, *Spodoptera frugiperda* (J E Smith), in maize in East Africa. Crop Prot. **105**, 10–15 (2018). https://doi.org/10.1016/j.cropro.2017.11.003
17. H. Izadi-Vasafi, F. Ghayoumi, S. Karbasizadeh-Esfahani, M. Ghafghazi, Comparing the effect of sodium-based and calcium-based crosslinkers on the swelling, mechanical and rheological properties of chitosan/gelatin/starch films. J. Macromol. Sci. Part B Phys. **59**, 331–343 (2020). https://doi.org/10.1080/00222348.2020.1714854
18. S. Kumar, A. Shukla, P.P. Baul, A. Mitra, D. Halder, Biodegradable hybrid nanocomposites of chitosan/gelatin and silver nanoparticles for active food packaging applications. Food Packag. Shelf Life **16**, 178–184 (2018). https://doi.org/10.1016/j.fpsl.2018.03.008
19. T.S.M. Kumar, N. Rajini, K. Obi Reddy, A. Varada Rajulu, S. Siengchin, N. Ayrilmis, All-cellulose composite films with cellulose matrix and Napier grass cellulose fibril fillers. Int. J. Biol. Macromol. **112**, 1310–1315 (2018). https://doi.org/10.1016/j.ijbiomac.2018.01.167
20. T.N.T. Rohadi, M.J.M. Ridzuan, M.S.A. Majid, A. Khasri, M.H. Sulaiman, Isolation and characterisation of cellulose from cortex, pith and whole of the *Pennisetum purpureum*: effect of sodium hydroxide concentration. J. Mater. Res. Technol. **9**, 15057–15071 (2020). https://doi.org/10.1016/j.jmrt.2020.10.102
21. A.T. Mart, A. Gutie, Structural characterization of the lignin in the cortex and pith of elephant grass (*Pennisetum purpureum*) stems. J. Agric. Food Chem. **60**, 3619–3634 (2012). https://doi.org/10.1021/jf300099g
22. S.T. Cholake, R. Rajarao, P. Henderson, R.R. Rajagopal, V. Sahajwalla, Composite panels obtained from automotive waste plastics and agricultural macadamia shell waste. J. Clean. Prod. **151**, 163–171 (2017). https://doi.org/10.1016/j.jclepro.2017.03.074
23. ASTM D882-02, Standard Test Method for Tensile Properties of Thin Plastic Sheeting. West Conshohocken, 2002. https://doi.org/10.1520/D0882-02

24. A.D. French, Increment in evolution of cellulose crystallinity analysis. Cellulose **27**, 5445–5448 (2020). https://doi.org/10.1007/s10570-020-03172-z
25. A.D. French, M. Santiago Cintrón, Cellulose polymorphy, crystallite size, and the Segal Crystallinity Index. Cellulose **20**, 583–588 (2013). https://doi.org/10.1007/s10570-012-9833-y
26. N. Ramakrishnan, S. Sharma, A. Gupta, B.Y. Alashwal, Keratin based bioplastic film from chicken feathers and its characterization. Int. J. Biol. Macromol. **111**, 352–358 (2018). https://doi.org/10.1016/j.ijbiomac.2018.01.037
27. M.R. Amin, M.A. Chowdhury, M.A. Kowser, Characterization and performance analysis of composite bioplastics synthesized using titanium dioxide nanoparticles with corn starch. Heliyon **5**, e02009 (2019). https://doi.org/10.1016/j.heliyon.2019.e02009
28. S.C. Koay, V. Subramanian, M.Y. Chan, M.M. Pang, K.Y. Tsai, K.H. Cheah, Preparation and characterization of wood plastic composite made up of durian husk fiber and recycled polystyrene foam. MATEC Web Conf. **152**, 02019 (2018). https://doi.org/10.1051/matecconf/201815202019
29. V. Bátori, M. Jabbari, D. Åkesson, P.R. Lennartsson, M.J. Taherzadeh, A. Zamani, Production of pectin-cellulose biofilms: a new approach for citrus waste recycling. Int. J. Polym. Sci. (2017). https://doi.org/10.1155/2017/9732329
30. R.F. Santana, R.C.F. Bonomo, O.R.R. Gandolfi, L.B. Rodrigues, L.S. Santos, A.C. Dos Santos Pires, C.M. Veloso, Characterization of starch-based bioplastics from jackfruit seed plasticized with glycerol. J. Food Sci. Technol. **55**, 278–286 (2018)
31. A.S. Giwa, H. Xu, J. Wu, Y. Li, F. Chang, X. Zhang, Z. Jin, B. Huang, K. Wang, Sustainable recycling of residues from the food waste (FW) composting plant via pyrolysis: thermal characterization and kinetic studies. J. Clean. Prod. **180**, 43–49 (2018). https://doi.org/10.1016/j.jclepro.2018.01.122
32. M. Lubis, M. Bangun Harahap, M. Hendra, S. Ginting, M. Sartika, H. Azmi, Production of bioplastic from avocado seed starch reinforced with microcrystalline cellulose from sugar palm fibers. J. Eng. Sci. Technol. **13**, 381–393 (2018)
33. A. Muhammad, A. Roslan, S.N.A. Sanusi, M.Q. Shahimi, N.Z. Nazari, Mechanical properties of bioplastic form cellulose nanocrystal (CNC) mangosteen peel using glycerol as plasticizer. J. Phys. Conf. Ser. **1349**, 12099 (2019). https://doi.org/10.1088/1742-6596/1349/1/012099
34. M.J.M. Ridzuan, M.S. Abdul Majid, A. Khasri, K.S. Basaruddin, A.G. Gibson, Effect of moisture exposure and elevated temperatures on impact response of *Pennisetum purpureum*/glass-reinforced epoxy (PGRE) hybrid composites. Compos. Part B Eng. **160**, 84–93 (2019). https://doi.org/10.1016/j.compositesb.2018.10.029
35. Isroi, A. Cifriadi, T. Panji, N.A. Wibowo, K. Syamsu, 2017. Bioplastic production from cellulose of oil palm empty fruit bunch, in: IOP Conf. Ser. Earth Environ. Sci. 65, 012011. https://doi.org/10.1088/1755-1315/65/1/012011
36. M.K. Marichelvam, M. Jawaid, M. Asim, Corn and rice starch-based bio-plastics as alternative packaging materials. Fibers **7**, 32 (2019). https://doi.org/10.3390/fib7040032
37. H. Hermansyah, R. Carissa, M.B. Faiz, P. Deni, Food grade bioplastic based on corn starch with banana pseudostem fibre/bacterial cellulose hybrid filler. Front. Chem. Eng. Metall. Eng. Mater. III **997**, 158–168 (2014). https://doi.org/10.4028/www.scientific.net/AMR.997.158
38. R. Gurram, P.F. Souza Filho, M.J. Taherzadeh, A. Zamani, A solvent-free approach for production of films from pectin and fungal biomass. J. Polym. Environ. **26**, 4282–4292 (2018). https://doi.org/10.1007/s10924-018-1300-x
39. N.A. Ismail, S. Mohd Tahir, N. Yahya, M.F. Abdul Wahid, N.E. Khairuddin, I. Hashim, N. Rosli, M.A. Abdullah, Synthesis and characterization of biodegradable starch-based bioplastics. Mater. Sci. Forum **846**, 673–678 (2016)
40. M.C. Etty, S. D'Auria, S. Shankar, S. Salmieri, J. Coutu, A. Baraketi, M. Jamshidan, C. Fraschini, M. Lacroix, New immobilization method of anti-PepD monoclonal antibodies for the detection of Listeria monocytogenes p60 protein—Part a: optimization of a crosslinked film support based on chitosan and cellulose nanocrystals (CNC). React. Funct. Polym. **146**, 104313 (2020). https://doi.org/10.1016/j.reactfunctpolym.2019.06.021
41. M.M. Siagian, P. Tarigan, Production of starch based bioplastic from cassava peel reinforced with microcrystalline celllulose avicel PH101 using sorbitol as plasticizer. J. Phys. Conf. Ser. (2016). https://doi.org/10.1088/1742-6596/710/1/012012
42. M. Prochoń, A. Marzec, B. Szadkowski, Preparation and characterization of new environmentally friendly starch-cellulose materials modified with casein or gelatin for agricultural applications. Materials (Basel). **12**, 1684 (2019)
43. X. Xu, J. Yu, C. Liu, G. Yang, L. Shi, X. Zhuang, Xanthated chitosan/cellulose sponges for the efficient removal of anionic and cationic dyes. React. Funct. Polym. **160**, 104840 (2021). https://doi.org/10.1016/j.reactfunctpolym.2021.104840
44. N.Johnsson, F. Steuer, Bioplastic material from microalgae extraction of starch and PHA from microalgae to create a bioplastic material, Degree Project Technology, 2018.
45. B. Jiang, S. Li, Y. Wu, J. Song, S. Chen, X. Li, H. Sun, Preparation and characterization of natural corn starch-based composite films reinforced by eggshell powder preparation and characterization of natural corn starch-based composite films reinforced by eggshell powder. CyTA-Journal Food **16**, 1045–1054 (2018). https://doi.org/10.1080/19476337.2018.1527783
46. A.D. French, Idealized powder diffraction patterns for cellulose polymorphs. Cellulose **21**, 885–896 (2014). https://doi.org/10.1007/s10570-013-0030-4
47. B.Y. Alashwal, M. Saad Bala, A. Gupta, S. Sharma, P. Mishra, Improved properties of keratin-based bioplastic film blended with microcrystalline cellulose: a comparative analysis. J. King Saud Univ. Sci. **32**, 853–857 (2020). https://doi.org/10.1016/j.jksus.2019.03.006